

Influence of the Cavitator and Nozzle Parameters on the Efficiency of Operation of a Generator of Pulsed Jets

S. A. Ocheretyani^{a,*} and V. V. Prokof'ev^{a,**}

^aMoscow State University, Institute of Mechanics, Moscow, Russia

*e-mail: ocheret@imec.msu.ru

**e-mail: vlad.prokof@yandex.ru

Received December 22, 2022; revised April 13, 2023; accepted June 6, 2023

Abstract—The regime of cavitation self-oscillations in a hydraulic system that contains a ventilated cavity with a negative cavitation number is used to create a generator of periodic impulse jets. The influence of the parameters of cavitator and output nozzle of the generator on the intensity of the impact of liquid outflowing on an obstacle (shield) located perpendicular to the direction of jet outflow is studied. It is found that increase in the nozzle length can significantly increase the efficiency of the generator, and a smooth constriction of the channel ahead of the cavitator can help to increase the operating range of the generator in the direction of larger gas blows. It is shown that there is a scale effect, namely, the relative intensity of self-oscillations decreases with increase in the liquid head pressure; however, it tends to reach a horizontal asymptote.

Keywords: jet flow, cavity, negative cavitation number, cavitation self-oscillations, pulsating technologies

DOI: 10.1134/S001546282360058X

Studies of fluid flows in the presence of a ventilated cavity with negative cavitation number, carried out at the Institute of Mechanics of Moscow State University [1–3], showed that cavitation self-oscillations with a high intensity of pressure fluctuations develop under certain conditions in the hydraulic system both in the cavity and in the upstream flow region. This regime can be used to create a pulsed jet generator. The most obvious application of such a generator can be found in water jet mining technologies. Modern investigations show that the performance of water jet technology grows rapidly with increase in the water pressure. However, obtaining stationary high-parameter jets is associated with great technical difficulties. Pulsating and pulsed jets of high-pressure liquid are becoming more and more widespread, their efficiency significantly exceeds stationary jets. Monograph [4] provides a review of studies on the problem of pulsed generation of high-pressure jets. To obtain jets with very high parameters, impulse water cannons are usually used (liquid receives an impulse due to the impact of a piston accelerated by powder gases) and hydraulic guns (liquid in the barrel accelerates along with the piston). Note that the closest relation to the topic considered in this paper is the scheme of a pistonless pulsed water jet, i.e., the liquid mass is accelerated directly by gas. Calculations and experiment [4, 5] showed that the velocity of such jets can reach 1600 m/s with a sufficiently large throw range when flowing both into air and into a space flooded with water. Note that the use of this method to create the periodic pulsed jet high parameter is difficult due to the complexity of “recharging” the device.

At more moderate velocities, the high-pressure hydraulic jets are used in the development of minerals such as coal and ore. Investigations into the methods of destruction of materials by jets, carried out by various scientific teams (see [6]), have shown that their efficiency strongly depends on the nature of the applied loads: static (continuous) or dynamic (pulsating) ones which are created by a liquid jet acting on the object being destroyed. Studies [6] have shown that there is a noticeable increase in the productivity of jet installations which use pulsating technologies, as well as a decrease in the specific energy intensity of the destruction of materials and a decrease in the water consumption. This ensures the acceptable moisture content of the extracted mineral. For the successful application of the hypopulse destruction method, which ensures the creation of repetitively variable loads, it is necessary to have efficient and easy-to-use devices that form pulsed jets of the required parameters. In [6], devices capable of providing a pulsating regime of jet installations were reviewed. In particular, an air pulsator, in which a flow discontinuity

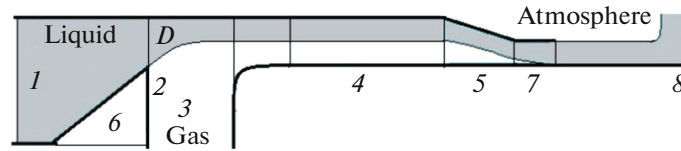


Fig. 1. Diagram of the plane jet facility.

is created due to periodic introduction of portions of air into the liquid jet, was described. As a rule, mechanical devices are used to organize pulsating operating regimes in such installations.

At present, examples of jet flow in hydraulic systems in which stable intense cavitation self-oscillating regimes take place at constant parameters of the supplied water and air without using any mechanical systems that excite oscillations are well known [2, 7]. A developed self-oscillating regime close to intermittent flow with a very low liquid consumption can be implemented under certain conditions. This regime can be used to organize the generation of periodic pulsed jets.

The study of the mechanism of self-oscillations showed that an important factor is the phase shift of pressure fluctuations in the prechamber and cavity; so, two pulses are formed at each period on the oscillogram of the pressure drop across the cavitator, namely, a positive pulse contributes to the outflow of a discrete liquid mass, while the outflow stops or even gas is released from the cavity into the prechamber due to a negative pulse (description and installation diagram see below in Section 1). In the present paper, we study self-oscillatory regimes in a hydraulic line containing a resistance (cavitator), a ventilated gas cavity, and a convergent channel (nozzle) through which liquid and gas flow into the atmosphere. Under moderate blowing, the gas cavity is kept in the area behind the cavitator, but with increase in air blowing, both the pulsations and the average pressure in the cavity increase and more and more significant amount of air is released into the area ahead of the cavitator, while self-oscillations continue, but there is a noticeable change in their parameters. An important parameter is the ratio of the hydraulic resistances of the cavitator and the nozzle. At the high cavitator resistance, when the width of the jet flowing into the cavity is less than the width of the minimum nozzle cross-section, self-oscillations are observed only under significant air blowing into the cavity. With decrease in the cavitator resistance, the oscillation regime with the release of gas into the supply water line shifts towards the smaller gas blows. The scale effect was studied in the range of fluid head pressures from 0.05 to 0.4 MPa. The experimental data showed that the intensity of pressure fluctuations in the cavity related to the head pressure decreases with increase in the pressure head, but tends to reach a horizontal asymptote. This is in good agreement with the results of theoretical calculations.

1. PLANE JET FACILITY

In Fig. 1 we have presented the diagram of a plane model of a cavitation pulse jet generator: the jet flows out of prechamber 1 through the gap $D = 10$ mm between the edge of cavitator 2 and the rectilinear channel wall. Ventilated gas cavity 3 is formed downstream of the cavitator. The facility nozzle consists of inlet part (circle with a radius of 10 mm), channel 4 with a width of $H_0 = 10$ mm and linearly convergent part 5 with the width of outlet cross-section $H_e = 6$ mm. There can be a confuser (6) ahead of the cavitator, and a collimator at the exit from the nozzle—constant cross-section nozzle 7. In Fig. 1 we have schematically shown a stationary ideal fluid flow with a cavity closing on the solid wall. The experimental data were obtained at the fluid head pressure of 0.1 MPa. The dependence of the impact intensity on the obstacle on the distance from the obstacle, as well as on the nozzle length (the length of the central part of the nozzle or the length of the end nozzle (collimator) was varied). We also studied the influence of the cavitator shape on the intensity of impact on the obstacle mounted perpendicular to the direction of the jet outflow from the generator. Oscillograms of pressure fluctuations were recorded in the prechamber, the cavity, and at corner point 8, where the impact interaction of the jet with the plane wall—obstacle (shield) 9—occurs (description of the experimental equipment is given in [8]).

The time-averaged pressures in the prechamber and cavity, as well as the flow rates measured under steady-state conditions in the lines supplying liquid and gas, were used as the hydraulic characteristics of flow. The leading frequency of self-oscillations was determined from the pressure oscillograms, as well as the intensity of pressure fluctuations averaged over the recording period of the oscillogram in the prechamber A_0 , the cavity A_c , and the intensity of shock pulses A_m at the corner point 8 of obstacle (see Fig. 1). The average amplitude of pressure pulsations was determined as follows: the difference between the max-

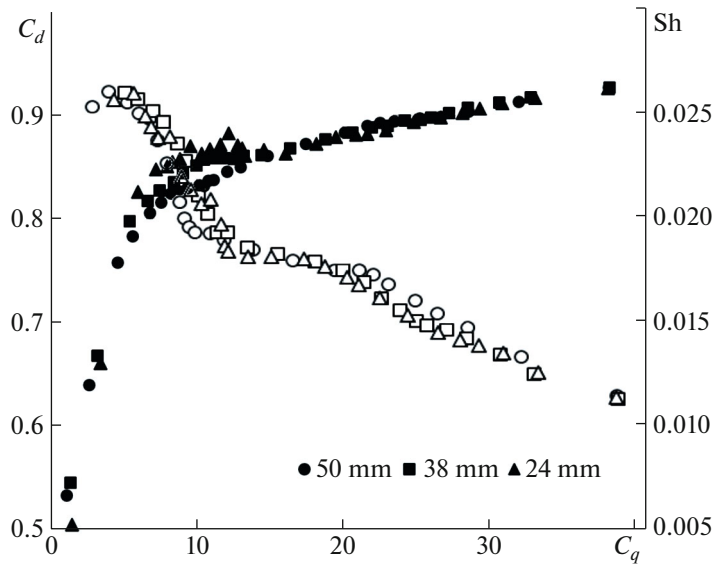


Fig. 2. Dependences of C_d on C_q (left scale, filled symbols) and Sh on C_q (right scale, hollow symbols) at the nozzle length of 30 mm, $P_0 = 0.1$ MPa, for three distances from the nozzle exit to the obstacle (24, 38, and 50 mm).

imum and minimum pressures was determined for each oscillation period, then the average value was found over all full periods of self-oscillations during the recording of the oscillogram (the recording time and the number of points were selected from the conditions so that the recording contained at least 10 self-oscillation periods and each pulse accounted for at least 10 recording points). Only the regimes of self-oscillations of the lowest, first mode were studied (see [8]).

The main dimensionless flow parameters are as follows: the pressure coefficient in the cavity C_d , the coefficient of gas injection into the cavity C_q , and the Strouhal number Sh:

$$C_d = \frac{\bar{p}_c - p_a}{\bar{p}_0 - p_a} = \frac{P_c}{P_0}, \quad C_q = \frac{Q_g}{Q_l}, \quad \text{Sh} = f \frac{D}{V_\infty}, \quad V_\infty = \sqrt{2P_0/\rho_l}.$$

Here, bar means the time-average quantity, p_c and p_0 are the pressures in the cavern and in the settling chamber, p_a is the atmospheric pressure, Q_g is the volumetric flow rate of the gas blown into the cavern at the pressure in the cavern, Q_l is the liquid flow rate, ρ_l is the liquid density, and f is the characteristic (leading) self-oscillation frequency.

The influence of the geometrical characteristics of the nozzle and cavitator was studied with the following quantities unchanged: the cavitator slot width ($D = 10$ mm), the inlet constriction (a circle with a radius of 10 mm), the width of the area of constant cross-section of 10 mm (4 in Fig. 1), the constant restriction of nozzle 5 from 10 to 6 mm; the self-oscillation regimes corresponded to the first (low-frequency) mode (see [8]). The efficiency of pulse generation for various flow regimes and for various parameters of the nozzle and cavitator was estimated only by comparing the values of A_m/P_0 .

2. JET RANGE

In Figs. 2 and 3 we have plotted the graphs of C_d , Sh, and the intensity of pressure pulsations A_c and A_m as functions of the blowing coefficient C_q for a nozzle with the total length of 30 mm (inlet constriction, section of constant cross-section, outlet constriction) at various distances from the nozzle exit to the obstacle: 24, 38, and 50 mm.

In the studied range of distances from the obstacle (approximately 4–8 diameters of the nozzle exit cross-section), this quantity has practically no effect on the characteristics of fluctuations in the nozzle. Depending on the amount of gas injection C_q , the nature of the flow changes significantly. At small blows ($C_q \sim 1$), the jet flows out of slot D (Fig. 1) almost stationary; as C_q increases, the cavity pressure (or the pressure coefficient C_d), as well as the intensity of pressure fluctuations in the cavity, begins to increase rapidly (Fig. 3a). The pulsation frequency decreases (Fig. 2). This can be explained by a decrease in the wave propagation velocity along the cavity boundary with increase in the pressure [8]. When the blowing

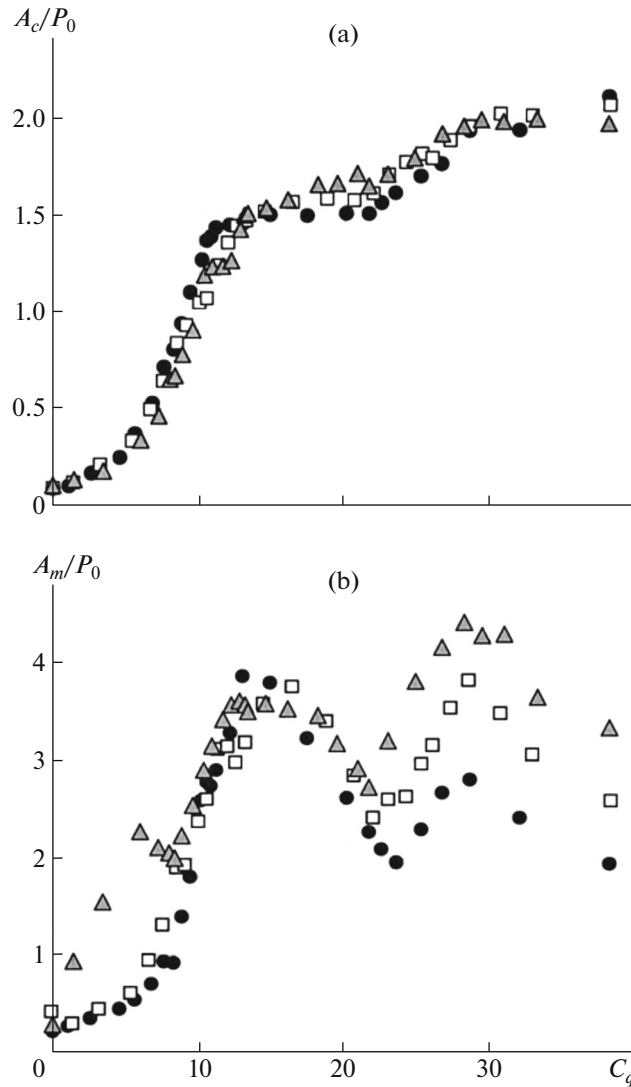


Fig. 3. Relative intensity of pressure pulsations in the cavity (a) and pressure shock pulses on the obstacle (b) as functions of the blowing coefficient at a nozzle length of 30 mm, $P_0 = 0.1$ MPa, for three distances from the nozzle exit to the obstacle (24, 38, and 50 mm). The same notation of points as in Fig. 2.

coefficient C_q is greater than 10, variations in these parameters slow down. For these injections, the cavity is no longer limited by the cavitator plane (2 in Fig. 1), namely, more and more intense gas ejections into the area ahead of the cavitator (into prechamber 1, Fig. 1) begin. This changes significantly the flow configuration. The intensity of pressure fluctuations in the cavity (Fig. 3a) increases monotonically with C_q , while the amplitude of impact of liquid portions on the obstacle (at point 8 in Fig. 1) has two maxima (Fig. 3b). The second maximum is located in the region of self-oscillations with significant gas ejections into the prechamber. It can be seen that the second maximum is greater than the first one for a distance to the obstacle of 25 mm. This can be explained by the effect of increase in the acceleration distance of the liquid portion due to the space displaced by the gas in prechamber, and the gas pressure in the cavity is higher here. It can be seen that the first maximum almost does not change with variation in the distance from 25 to 50 mm, while the second maximum decreases rapidly with the distance of the obstacle from the nozzle exit, and at a distance of 50 mm it is already noticeably smaller than the first maximum. This indicates a significant perturbation of jet flow in the presence of ejections into the prechamber; as a result, the range of the jet facility in the regime of the absence of ejections into the prechamber is much higher than in the presence of ejections. However, from the point of view of increase in the impact on the obstacle, the second regime is promising, at least when using small distances from the nozzle exit to the obstacle.

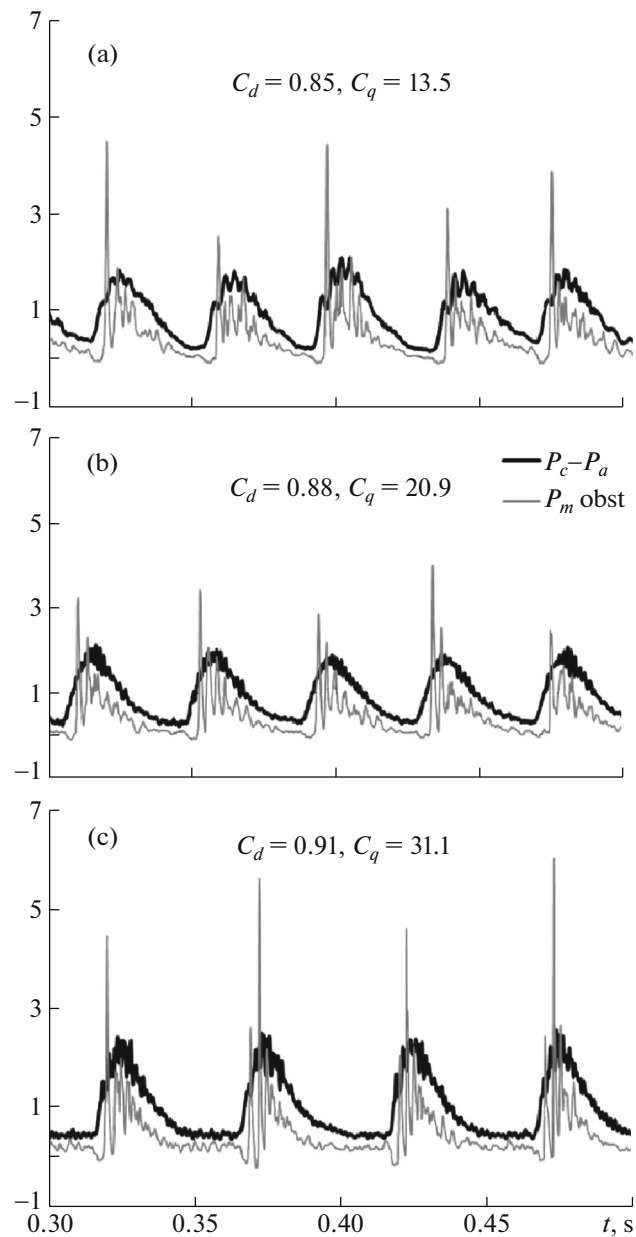


Fig. 4. Oscillograms of pressure fluctuations in the cavity (thick curves) and at the corner point of the obstacle (thin curves) for a nozzle 30 mm long, at a distance from the obstacle of 25 mm for various values of C_d and C_q . The head pressure $P_0 = 0.1$ MPa.

Figures 4 and 5 show fragments of oscillograms (with duration of 0.2 s) of the pressure fluctuations in the cavity p_c and at the corner point of the obstacle p_m at $P_0 = 0.1$ MPa for two distances from the nozzle exit to the obstacle: 25 and 50 mm. The recording duration of each regime was 1 s, the recording time step was 10^{-4} s. It can be seen that for the presented cases, the pressure oscillations in the cavity are close to periodic, the pressure pulses on the obstacle have the shock nature, and their amplitude has a significant spread. The oscillograms in Figs. 4 and 5 were obtained for various blowing values and correspond to the regions of the first maximum, the minimum, and the second maximum of the average amplitude of shock pulses (see Fig. 3b). For an obstacle distance of 25 mm, the pulsation amplitude for the second maximum (Fig. 4c, thin lines) is higher than that for the first maximum (Fig. 4a). It can be seen that the impact interaction of the jet with the obstacle generates a whole sequence of short pulses. For self-oscillations without gas ejections into the prechamber, the first pulse has the highest amplitude, followed by a sequence of damped pulses; in the presence of ejections, this is not the case. The oscillograms for a distance of 50 mm

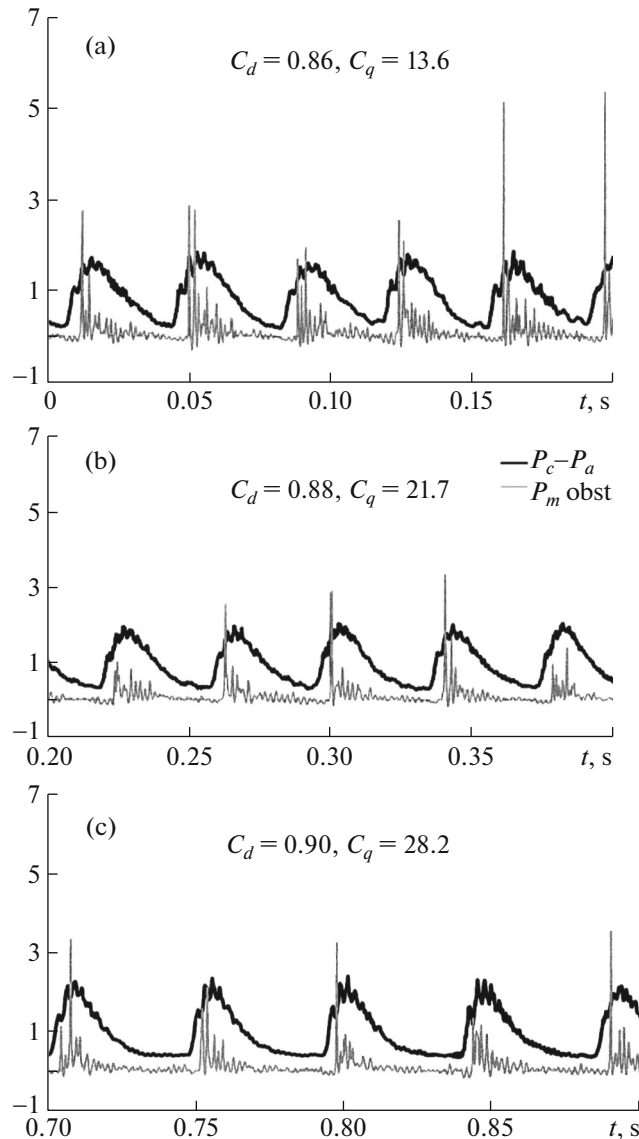


Fig. 5. Oscillograms of pressure fluctuations in the cavity (thick curves) and at the corner point of the obstacle (thin curves) for a nozzle 30 mm long, at a distance from the obstacle of 50 mm for various values of C_d and C_q . The head pressure $P_0 = 0.1$ MPa.

(Fig. 5a) show that the nature of impact of the jets on the obstacle for the regime without ejections has almost not changed. For the second regime (Fig. 5c), the pulse amplitude drops significantly.

Thus, in the self-oscillation regime without gas ejection into the prechamber, more stable liquid jets are obtained; however, the second regime also deserves attention, since here it is possible to obtain a more intense effect at small distances from the obstacle.

3. EFFECT OF NOZZLE LENGTH

We have carried out comparative studies of three nozzles, namely, two nozzles with a length of 55 mm and a nozzle with a length of 30 mm (the length was varied by varying the length of the middle boost section). The third nozzle also had a length of 55 mm, the shape of its flow part coincided with the 30 mm nozzle, but behind constriction 5 (see Fig. 1) there was a section of constant cross-section—collimator 7 (Fig. 1), 6 mm wide and 25 mm long. In [5], the beneficial effect of the collimator on the intensity of impact on the obstacle of the jet flowing from the hydrogun nozzle was noted.

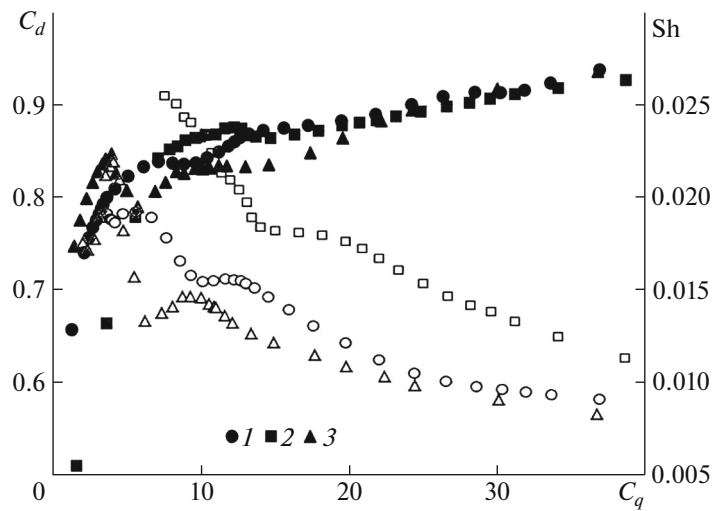


Fig. 6. Dependences of C_d on C_q (left scale, filled symbols) and Sh on C_q (right scale, hollow symbols) for the nozzles 55 and 30 mm long, as well as 30 mm long with the collimator of 25 mm (1, 2, and 3, respectively). The head pressure $P_0 = 0.1$ MPa.

In Figs. 6 and 7 we have shown the dependences of C_d , Sh , and the intensity of the pressure pulsations A_c and A_m on the blowing coefficient C_q for a nozzle 55 and 30 mm long and 30 mm long with a 25 mm collimator (curve 1, 2, and 3, respectively). If we compare curves 1 and 2, it can be seen that the average pressure in the cavity varies only slightly with increase in the length of the accelerating section, the pressure pulsation intensity slightly increases, the pulsation frequency drops significantly (by 1.5–2 times), and the intensity of the impact on the obstacle significantly increases. The presence of the collimator also reduces the self-oscillation frequency and increases the impact on the obstacle (if we compare curves 2 and 3 in Fig. 7). Moreover, in the regime of no gas ejections behind the cavitator, an increase in the nozzle length due to the accelerating section or the collimator (curves 1 and 3 in Fig. 11) gives approximately the same effect of increasing the shock pressure on the obstacle, and in the presence of ejections (with increase in the blowing intensity), the collimator efficiency decreases noticeably.

In Fig. 8 we have reproduced the calculated dependences of the velocity (a) of the front boundary of the liquid portion moving in the nozzle channel and the pressure in the cavity $(p_c - p_a)/P_0$ (b) on the coordinate of this boundary X/D for the same three configurations with the same numeration of curves as that in Fig. 6. Here, $X/D = 0$ is the nozzle entry coordinate, $X/D = 3$ or 5.5 is the exit cross-section coordinate for the nozzles with a length of 30 or 55 mm. The theoretical model [8] does not take into account the effect of gas ejections behind the cavitator; therefore, for analysis, we took the gas flow rate coefficient $C_q = 15$ at which intense self-oscillations take place, but there are still no significant gas ejections behind the cavitator. The corresponding values of C_d and Sh , which determine the initial velocity of the liquid portion and its mass, were taken based on the data in Figs. 8 and 9. It can be seen that the velocity of the front boundary of the liquid portion at the exit for a 55 mm long nozzle is noticeably higher than that for a 30 mm long one (curves 1 and 2 in Fig. 8a). From a comparison of curves 1 and 3 in the same figure we can see that at the exit from the collimator, due to losses in the narrow channel, the velocity of the liquid boundary is close to the velocity at the exit from the short nozzle. Nevertheless, the experiment shows that the presence of the collimator increases the impact on the obstacle. Possible, this is due to increase in the mass of liquid which has a high velocity at the nozzle outlet (in our case, the total mass of the liquid portion also increases due to decrease in the frequency of self-oscillations, see Fig. 6). In Fig. 8b we have plotted the graphs of pressure growth in the cavity as a function of the coordinate of the front boundary of the liquid portion in the nozzle. Qualitatively, the picture corresponds to the graphs in Fig. 7a, namely, the fastest increase in pressure in the cavity is observed in the case of the nozzle with collimator. The fact that at the instant when the liquid boundary reaches the exit cross-section of the nozzle in Fig. 8b the cavity pressure is slightly lower than the real amplitude of pressure fluctuations in the cavity can be explained by the fact that the calculation process was stopped at the instant when the boundary of the liquid portion reached the nozzle exit.

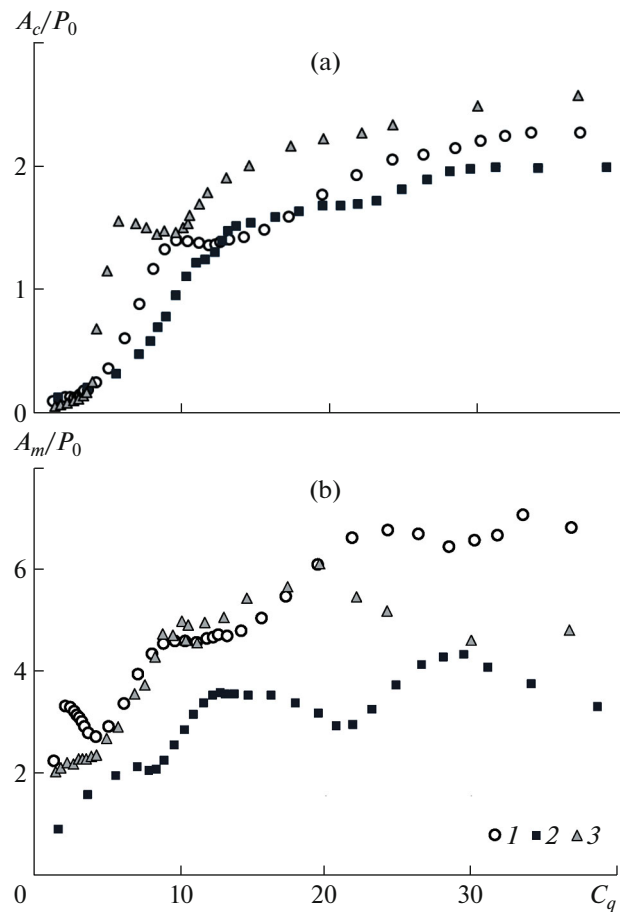


Fig. 7. Relative intensity of pressure fluctuations in the cavity (a) and impact pressure pulses on the obstacle (b) as functions of the blowing coefficient for the same conditions as those in Fig. 6.

4. CONFUSOR EFFECT

It was noted above that the flow regime with an ejection into the region ahead of the cavitator is of interest from the point of view of obtaining the maximum impact of the jets on the obstacle. The data in Fig. 3b indicate a decrease in the jet range in this regime. A series of experiments was carried out to determine the effect of linear confuser ahead of the cavitator on the formation of pulsed jets. The width of the flow path between the cavitator and the chamber wall remained unchanged ($D = 10$ mm), a nozzle 55 mm long was used (1 in Fig. 6), the distance from the nozzle exit to the obstacle was equal to 25 mm. With increase in the confuser length (decrease in the angle of constriction), the thickness of the jet flowing out into the cavity also increases, but the losses associated with increase in the resistance of the confuser increase (see [9]).

In Figs. 9–10 we have reproduced the dependences of C_d , Sh , and the intensity of pressure fluctuations A_c and A_m on the gas injection coefficient C_q for confusers with the constriction angles of 90° , 27° , and 11° . The data in Figs. 9 and 10 show that the intense self-oscillating regimes begin to develop earlier in the presence of the confuser. The frequency of self-oscillations decreases somewhat, which may be due to an increase in the thickness of the jet flowing into the cavity, while the intensity of self-oscillations increases. For a confuser with the constriction taper angle of 27° , a noticeable increase in the average amplitude of the pressure pulses on the obstacle as compared to the plate cavitator (90°) is observed in almost the entire blowing range, see Fig. 10b. For the longest confuser (11°), an increase in the average amplitude of the pressure pulses on the obstacle is observed in comparison with the plate only in the first of the regimes mentioned above. Thus, the use of the cavitator with a smooth restriction (confuser) can significantly increase the amplitude of the pulsed action of the generator on the obstacle.

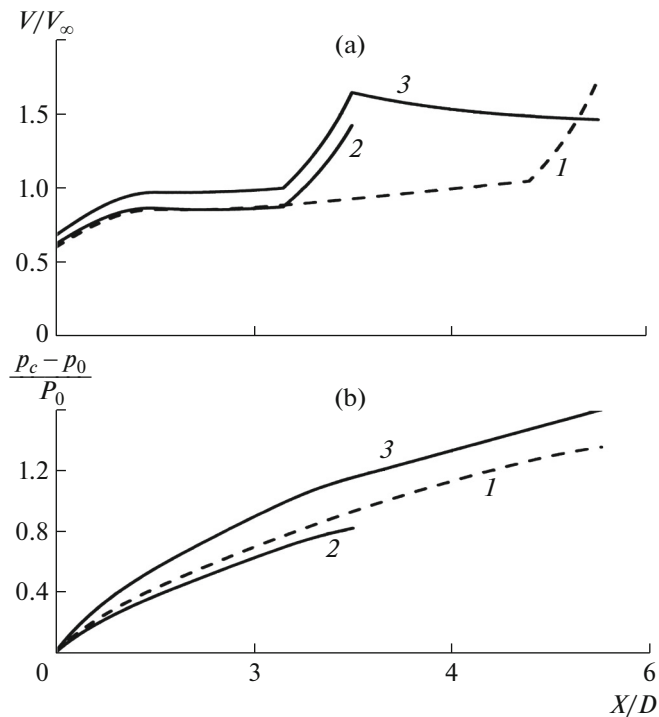


Fig. 8. Calculated dependences of the velocity V/V_∞ (a) and pressure $(p_c - p_a)/P_0$ (b) on the X/D coordinate of the front boundary of the liquid portion moving through the nozzle channel under the same conditions as in Fig. 6 (with the same numbering of curves).

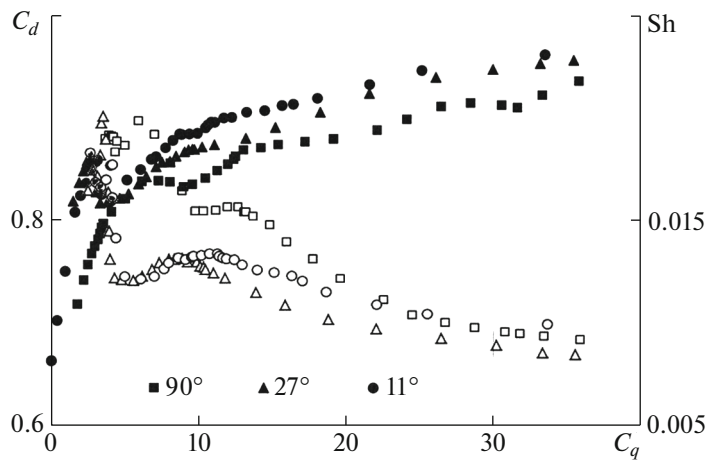


Fig. 9. Dependences of C_d on C_q (left scale, filled symbols) and Sh on C_q (right scale, hollow symbols) for the nozzle 55 mm long (curve 1 in Fig. 6) in the presence of a linear confuser with angles of restriction 90° , 27° , and 11° ahead of the cavitator.

5. EFFECT OF THE CAVITATOR RESISTANCE

From the above it follows that with increase in gas blowing into the cavern, the operation regime of the pulse jet generator switches at some instant to the self-oscillation regime with periodic gas ejection into the region ahead of the cavitator. This instant is primarily determined by the ratio of the hydraulic resistances of the cavitator and nozzle.

In Figs. 11 and 12 we have presented the characteristics of the flow in the pulse jet generator at fixed nozzle parameters (length 55 mm, similar to 1 in Fig. 6) and a distance from the nozzle exit to the obstacle

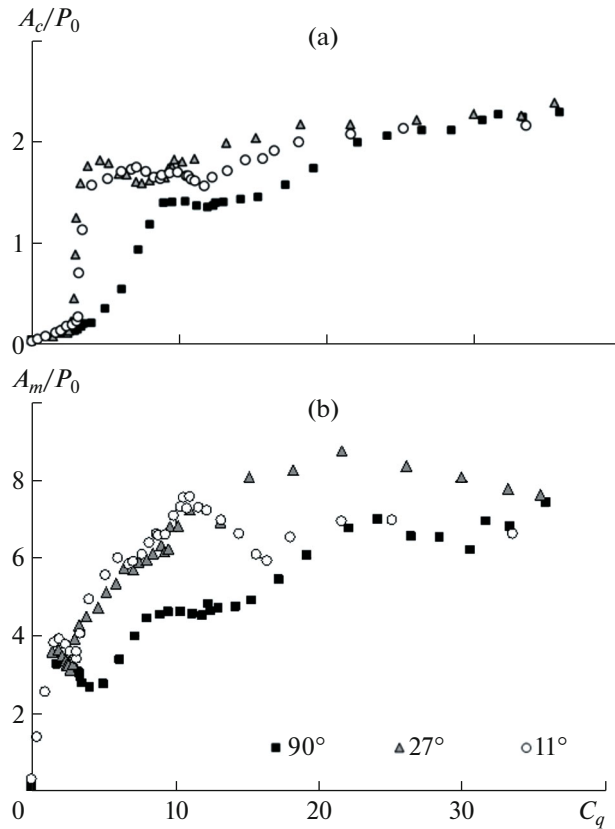


Fig. 10. Relative intensity of pressure fluctuations in the cavity (a) and pressure shock pulses on the obstacle (b) as functions of the blowing coefficient under the same conditions as in Fig. 9.

of 25 mm at various cavitator resistances. This was achieved mainly by changing the gap width $D = 23, 10,$ and 5 mm. In the first two cases, a plate cavitator (angle 90°) was used, in the last case we used a linear confuser with an angle of inclination 33.7° . Here, as the characteristic of the jet flowing into the cavity through the gap D , it is convenient to take its width H_j far from the cavitator, which was calculated, within the framework of the ideal fluid theory, from the measured fluid flow rate and the pressure in the cavity in the stationary flow regime without gas injection. In Figs. 11 and 12 curves 1–3 correspond to $H_j = 15.1, 6.6,$ and 4.4 mm, respectively.

Increase in the cavitator resistance leads to a delay in the transition to the regime with gas ejection into the region ahead of the cavitator, while a thinner jet flows into the cavity. At $H_j = 4.4$ mm (curve 3 in Figs. 11 and 12), the jet width is less than the minimum nozzle width (outflow can occur without interaction with the nozzle walls); however, the development of oscillations still begins, but at the higher gas flow rates, and the oscillation and shock impulse amplitudes A_c and A_m are much less than in other cases. At $H_j = 6.6$ mm (curve 2), the jet width is somewhat greater than the minimum nozzle width. Here, the pressure fluctuations in the cavity and the amplitude of shock pressures on the obstacle increase significantly as compared to a thinner jet. With further increase in the jet width (1 in Fig. 12), gas ejections behind the cavitator begin even at smaller blows, the pressure pulsations in the cavity increase, but the shock pulse amplitude A_m increases only slightly (see Fig. 12). In Fig. 11 we have plotted the graphs for the number Sh_j , in which the characteristic jet width H_j is used as the characteristic length. The closeness of the values of this number in the region of developed self-oscillations ($C_q = 8–15$) for all three cases (see Fig. 11) demonstrates that the frequency here is approximately inversely proportional to the jet width H_j .

6. SCALE EFFECT

All the experimental data presented above were obtained for the head pressure $P_0 = 0.1$ MPa. Previously, it was shown [8] that, depending on the flow velocity, there is a scale effect; i.e., the dimensionless

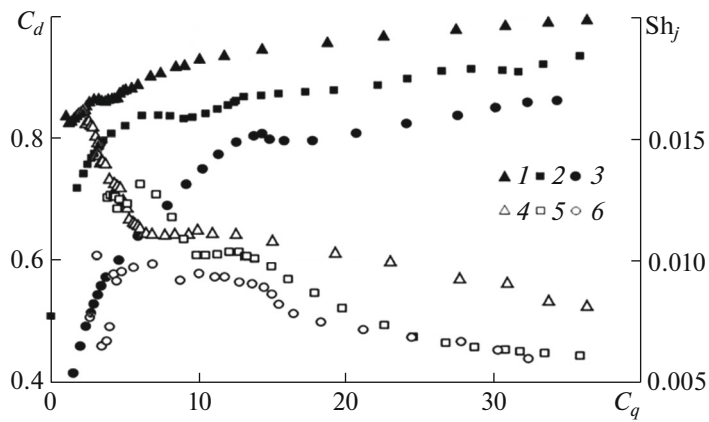


Fig. 11. Dependences of C_d on C_q (left scale, filled symbols) and Sh on C_q (right scale, hollow symbols) for the nozzle 55 mm long (without collimator), the distance to the obstacle is equal to 25 mm for various values of D and various characteristic widths of the jet flowing into the cavity $H_j = 15.1, 6.6,$ and 4.4 mm (curves 1–3 and 4–6, respectively).

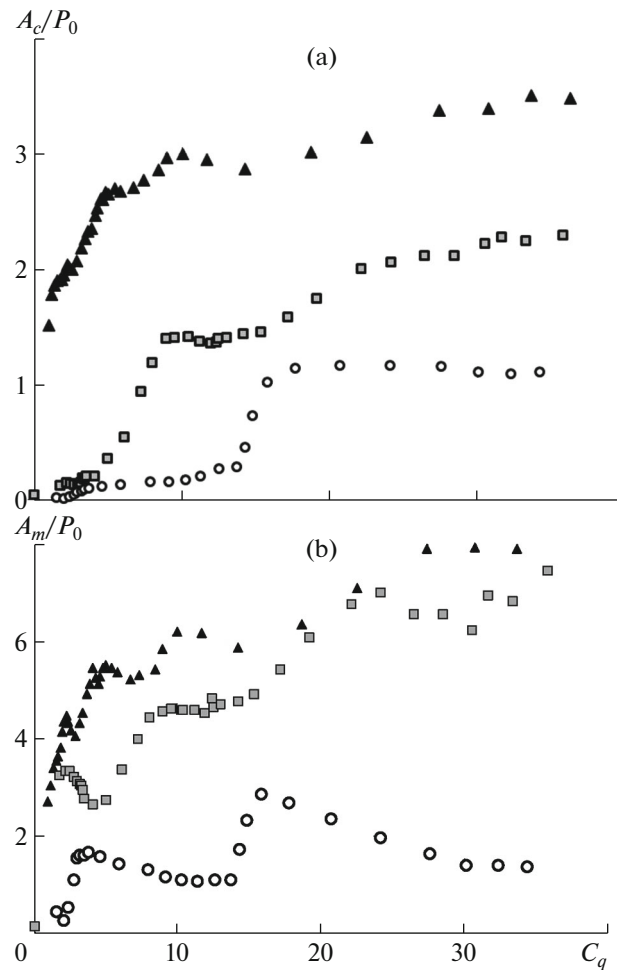


Fig. 12. Relative intensity of pressure fluctuations in the cavity (a) and pressure shock pulses on the obstacle (b) as functions of the blowing coefficient under the same conditions as in Fig. 11.

parameters of self-oscillations A_c/P_0 depend on P_0 . We studied the dependence of the dimensionless characteristics of pressure fluctuations on P_0 for a nozzle with the total length of 55 mm (a nozzle 30 mm long and a collimator 25 mm long) in the range of the head pressures P_0 from 0.05 to 0.4 MPa.

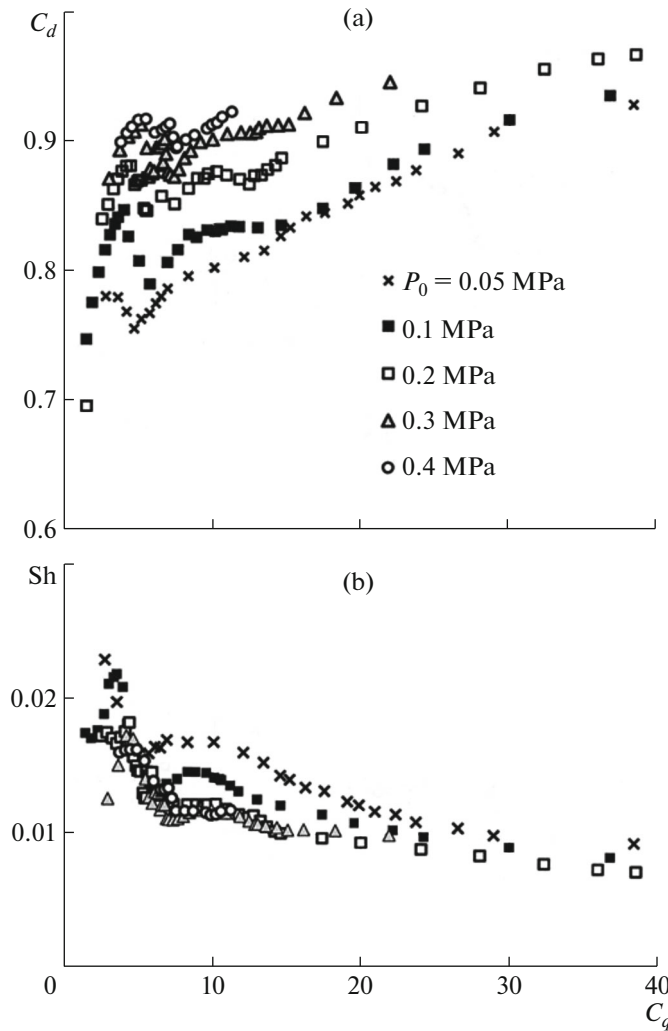


Fig. 13. Dependences of C_d (a) and Sh (b) on C_q for the nozzle of total length 55 mm (with a collimator of length 25 mm) at various head pressures P_0 .

The scale effect is already visible in Fig. 13 in which we have plotted C_d and Sh as functions of C_q . With increase in the head pressure P_0 , the pressure coefficient at a fixed C_q also increases (see Fig. 13a). Thus, the transition of self-oscillations to the regime with gas ejection behind the cavitator will occur at lower values of the volume flow rate coefficient C_q . However, as P_0 increases, the scale effect reduces. The data for the Strouhal number (Fig. 13b) show that at P_0 greater than 0.2 MPa, the change becomes insignificant. The scale effect affects stronger the level of the relative pressure fluctuations A_c/P_0 , which decreases with increase in P_0 (see Fig. 14). In addition, measurements of the intensity of pressure oscillations in the cavity showed that the range of existence of self-oscillations, if it is estimated in terms of C_q , decreases significantly with increase in P_0 . In Fig. 14 along the horizontal axis we have plotted the relative mass flow rates of gas $C_m = M_g/M_l = (\rho_{gc}/\rho_l)C_q$ instead of the relative volumetric flow rate C_q (M_g and ρ_{gc} are the mass flow rate of gas and the gas density at an average pressure in the cavity, M_l and ρ_l are the mass flow rate and density of liquid in the facility). In terms of the mass flow rate coefficient C_m , the range of existence of stable self-oscillations is retained with increase in the pressure. This may testify that the self-oscillatory regimes will persist with increase in P_0 while maintaining the relative mass flow rate of gas and liquid. In addition, as P_0 increases, the reduction in the relative value of the pressure fluctuations in the cavity slows down.

In Fig. 15 we have reproduced the theoretical dependences of the relative intensity of pressure fluctuations in the cavity on the head pressure for various initial volumes of the cavity (curves 1, 2, and 3 corre-

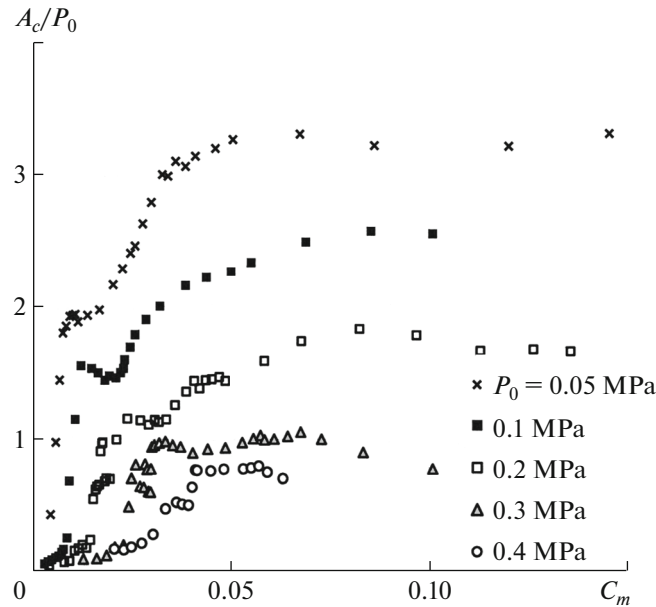


Fig. 14. Relative intensity of pressure fluctuations in the cavity for the nozzle of total length 55 mm (with a collimator of length 25 mm) at various head pressures P_0 .

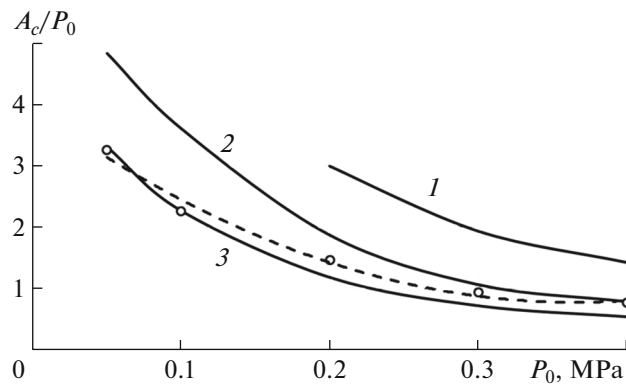


Fig. 15. Theoretical dependences of A_c/P_0 on the head pressure P_0 at $C_m = 0.05$ for the initial volumes of the cavity 2×10^{-3} , 3×10^{-3} , and $4 \times 10^{-3} \text{ m}^3$ (curves 1, 2, and 3, respectively). Comparison with the experimental data (dashed curve).

respond to 2×10^{-3} , 3×10^{-3} , and $4 \times 10^{-3} \text{ m}^3$, respectively). A one-dimensional model of the surge regime [8] was used. The maximum pressure in the cavity was taken to be the maximum pressure in the time interval limited from above by the instant of reaching the front boundary of the liquid portion of the outlet nozzle cross-section. In the calculations, the initial velocity and the mass of the liquid portion were set according to the C_d and Sh measured experimentally at $C_m = 0.05$. In addition, in Fig. 15 we have also reproduced the pressure fluctuation intensities measured in the cavity at $C_m = 0.05$ for the cavity volume $\sim 10^{-3} \text{ m}^3$. We can see a qualitative agreement between the experimental and calculated curves. The theory and the experiment show the effect of reducing the relative pressure fluctuations in the cavity with increase in the head pressure P_0 ; however, theoretical calculations have shown (see [8]) that at $C_q = \text{const}$ the dependences tend to a horizontal asymptote. It can be seen (Fig. 15) that the trend towards the horizontal asymptote also takes place in practice. However, the question of the generator operation at high pressures requires further study.

7. SUMMARY

The self-oscillatory flow regimes in a hydraulic line containing a resistance (cavitator), a ventilated gas cavity and a narrowing channel (nozzle) through which liquid and gas flow into the atmosphere has been

studied. The possibility of using the self-oscillation regime to create periodic pulsed jets is shown. In contrast to the well-known pulse installations, the periodic regime of intermittent liquid flow is implemented here at constant parameters of the liquid and gas supplied to the system without using any mechanical devices.

It was found that in the region of developed self-oscillations there are two different flow regimes, namely, a regime in which the cavity is limited by the cavitator cross-section in the process of pulsations (under moderate blowing) and, with an increase in blowing, a regime with intense gas ejections into the area ahead of the cavitator (into the prechamber) develops. It is shown that the range of the pulsed jet flowing out of the nozzle into the atmosphere decreases noticeably in this regime, in comparison with the regime without ejections beyond the cavitator. However, at short distances (up to 4 diameters of the nozzle exit cross-section), the intensity of the pressure pulses on the obstacle in the second regime exceeds the regime without gas ejections into the area ahead of the cavitator. It is shown that the smooth channel restriction ahead of the cavitator can contribute to significant increase in the amplitude of pressure pulses on the obstacle. The studies have shown that an increase in the nozzle length (increase in the length both due to the central insert and due to the use of a collimator at exit from the nozzle was considered) contributes to the increase in the amplitude of shock pulses on the obstacle.

The scale effect was studied in the range of the fluid head pressures from 0.05 to 0.4 MPa. The experimental data showed that the intensity of pressure fluctuations in the cavity, related to the head pressure, decreases with increase in the pressure but tends to reach a horizontal asymptote, which is consistent with the results of theoretical calculations.

REFERENCES

1. Kozlov, I.I. and Prokof'ev, V.V., Development of waves on a cavity surface with a negative cavitation number, *Doklady Physics*, 2006, vol. 56, no. 7, pp. 361–364.
2. Kozlov, I.I., Ocheretyanyi, S.A., and Prokof'ev, V.V., Self-oscillation regimes in a liquid jet curtain separating gas regions with different pressures, *Fluid Dyn.*, 2013, vol. 48, no. 6, pp. 738–746.
3. Ocheretyanyi, S.A. and Prokof'ev, V.V., Nozzle contraction effect on the performance of the generator of periodic pulsed jets, *Fluid Dyn.*, 2022, vol. 57, no. 2, pp. 122–134. <https://doi.org/10.1134/S0015462822020069>
4. Semko, A.N., *Impul'snyye strui zhidkosti vysokoy skorosti i ikh primeneniye: monografiya* (High-Velocity Pulsed Liquid Jets and Their Application), Ed. by Semko, A.N., Donetsk: DonNU, 2014.
5. Atanov, G.A. and Semko, A.N., Numerical analysis of the jet flows of compressible water, in: *Proc. of International Summer Scientific School "High Speed Hydrodynamics", June 2004, Cheboksary*, Computational Publications, Russia, 2004, pp. 39–44.
6. Savchenko, N.V. and Yakhno, O.M., Hydrodynamic approaches to the formation of pulsed jet for hydraulic destruction of solid materials, *Vestnik Sumsk. Gos. Univ. Ser. Tekhn. Nauki*, 2003, no. 12 (58), pp. 92–98.
7. Shkapov, P.M., Blagoveshchenskii, I.G., Gartig, E.B., and Doroshenko S.A., On the hysteresis nature of the development of self-oscillations in a hydraulic line with a limited artificial gas cavity at the outlet, *Nauka i obrazovanie*, Electronic sci.-tech. ed. MGTU im. N.E. Bauman, 2013, no. 10, pp. 1–10.
8. Prokof'ev, V.V., Ocheretyanyi, S.A., and Yakovlev, E.A., Using cavitation self-oscillation regimes to generate periodic pulsed jets, *J. Appl. Mech. Techn. Phys.*, 2021, vol. 62, no. 1, pp. 86–95.
9. Idel'chik, I.E., *Spravochnik po gidravlicheskim soprotivleniyam* (Handbook on Hydraulic Resistances), Moscow–Leningrad: Gosenergoizdat, 1960.

Translated by E.A. Pushkar